Influence of speed and flux estimation by Luenberger observer on IM drive with DTC

Karlovský Pavel, Lettl Jiří
Department of Electric Drives and Traction
FEE, Czech Technical University in Prague
Czech Republic
karlopav@fel.cvut.cz

Abstract—**The direct torque control (DTC) strategy is one of the most performance methods for induction machine (IM) drive torque control. The controlled stator magnetic flux and torque cannot be easily measured and therefore must be calculated using an IM mathematical model. This paper examines the impact of the replacement the original voltage IM model by Luenberger observer on the drive performance. As the original model requires only voltage and current, the observer is implemented in such a way that the same input variables can be used. The models are created and tests are carried out experimentally employing the dSPACE platform on induction motor of power 5.5 kW. The experimental results indicate better performance of the control strategy based on Luenberger observer.**

Keywords—induction motor drive; DTC; IM model; Luenberger observer

I. Introduction

The induction motor (IM) drive is used in many areas where the speed or torque control is required. And often, especially in the field of higher power, very accurate control is required. A lot of control strategies have been developed. The field oriented control (FOC) and direct torque control (DTC) [1] are utilized and they became an industrial standard. Both of them achieve high performance, but also suffer from certain disadvantages [2], [3]. This paper focuses on the DTC.

In the DTC, the stator flux and developed torque are controlled. These variables are not subjects of measurement and they must be calculated. As the induction motor is a nonlinear system it is hard to put together the model. Several models to describe the induction motor have ben developed. The most widely known are the voltage models, current models, observers, Kalman filters, etc. The DTC strategy usually utilizes the voltage model, as it is easy to implement. However, in a lot of working points the accuracy is not sufficient. It has been many attempts to improve the model accuracy. Most of them added filters for DC component or used transfer function instead of pure integrators [4], [5]. At DTC, the current models are utilized only rarely. Such model relies on the speed sensor, which the DTC itself does not need. It is used only in a few applications [6]. Observers and Kalman filters calculate the states of the system, in this case the flux and current [7], [8]. They usually require knowledge of the angular speed value, but very often they are utilized in order to estimate the angular speed value. Then the angular speed is treated as parameter that is being estimated by appropriate adaptive mechanism [3].

This paper focuses on Luenberger observer [9]. It is a specific kind of observer that corrects the estimated states through the feedback from the original system. This observer replaces the most widely used voltage model of the induction motor. To guarantee working on the same hardware system, the angular speed is not measured but estimated by the observer. Then influences of the estimated angular speed and flux values on a drive behavior are examined.

In the paper, the DTC is presented and the voltage model of the IM and Luenberger observer are explained at first. Then they are implemented on the drive and the tests are run. Finally, obtained results are presented and discussed.

II. Methods

In this chapter at first, the description of utilized DTC strategy with its original model of the IM is provided. Then the Luenberger observer calculating the same variables as the original model is explained.

A. DTC Strategy

In case of an induction motor drive the direct torque control strategy controls separately the torque developed by the motor and amplitude of the stator magnetic flux. These variables are calculated from the IM model. Hysteresis controllers are usually utilized to ensure the torque and flux amplitude values are close to their references.

In the motor, two magnetic flux vectors can be distingushed. Current flowing through the stator winding creates the stator flux vector and current in the rotor winding creates the rotor flux vector. The developed torque is directly proportional to their vector product. This also means that the torque is directly proportional to the amplitudes of the fluxes and to the angle between these vectors. This is expressed in (1) as follows.

ISBN 978-80-261-0642-5, © University of West Bohemia, 2017

$$T = \frac{L_m}{L_\sigma} \cdot p_p \cdot \psi_s \times \psi_r = \frac{L_m}{L_\sigma} \cdot p_p \cdot |\psi_s| \cdot |\psi_r| \cdot \sin\theta_{sr} \quad (1)$$

Here T is generated torque, L_m is magnetizing inductance, L_σ is leakage inductance, p_p is number of pole-pairs, $\boldsymbol{\psi_r}$ is rotor flux vector, $\boldsymbol{\psi_s}$ is stator flux vector and θ_{sr} is angle between flux vectors.

In induction motor, requirement on constant flux amplitude is common. Then changing angle $_{sr}$ between the flux vectors changes also the torque. The smallest torque is developed when difference angle is zero and the biggest one is developed when the vectors are perpendicular. The value of the angle is forced to stay within borders during DTC operation. Therefore, the developed torque is kept in certain borders, too.

The power inverter creates six active voltage vectors and two passive voltage vectors on its output. The stator flux is the integral of the voltage vector, which gives six possible direction of the flux vector change. Fig. 1 depicts the magnetic fluxes and voltage vectors in αβ orthogonal coordinates.

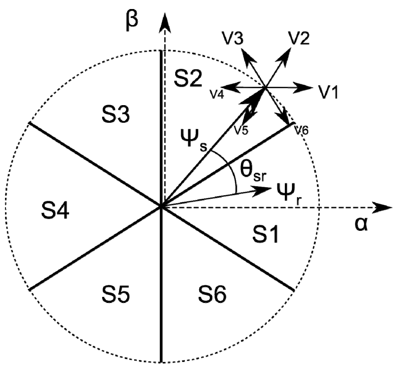

Figure 1. Effects of voltage vectors (V1 – V6) in flux sectors (S1 – S6) displayed in the αβ plane

Therefore, by applying any vector on the inverter, the certain response occurs. For example, in the figure the voltage vector V3 does not change the flux amplitude (or increases by a very small value) and increases torque (the angle between flux vectors increases) and V4 increases torque and decreases flux. The whole plane is divided into sectors and for each sector the table with responses can be defined as in Table I. From this switching table, the appropriate vector is chosen.

TABLE I. SWITCHING TABLE

ψ	T	Sector 1	Sector 2	Sector 3	Sector 4	Sector 5	Sector 6
	1	V_2(110)	V_3(010)	V_4(011)	V_5(001)	V_6(101)	V_1(100)
1	0	V_7(111)	V_0(000)	V_7(111)	V_0(000)	V_7(111)	V_0(000)
	-1	V_6(101)	V_1(100)	V_2(110)	V_3(010)	V_4(011)	V_5(001)
	1	V_3(010)	V_4(011)	V_5(001)	V_6(101)	V_1(100)	V_2(110)
0	0	V_0(000)	V_7(111)	V_0(000)	V_7(111)	V_0(000)	V_7(111)
	-1	V_5(001)	V_6(101)	V_1(100)	V_2(110)	V_3(010)	V_4(011)

The controlled variables are the stator flux vector and developed torque. The utilized IM model is based on the voltage model and the measured variables are voltage and current. Then the flux is calculated as integral of stator voltage subtracted by the voltage drop on winding (2) and the developed torque as cross product of current and flux vector (3).

$$\psi_s = \int (v_s - R_s \cdot i_s) dt \quad (2)$$

$$T = \frac{3}{2} \cdot p_p \cdot (\psi_{s\alpha} \cdot i_{s\beta} - \psi_{s\beta} \cdot i_{s\alpha}) \quad (3)$$

Here $\boldsymbol{v_s}$ is the stator voltage, R_s is resistance of the stator winding, and $\boldsymbol{i_s}$ is the current vector.

The advantage of the model is its easy implementation and required knowledge of only one parameter of the motor - the resistance of stator winding R_s. The disadvantage is the integration, which is prone to DC offset and low robustness towards measured noise.

B. Luenberger Observer

Unlike the voltage model, the Luenberger observer duplicates the whole system and calculates all variables. Further, the states of the system are corrected through the negative feedback of the comparison between the original system and the observer output. Usually, the input of the system is voltage vector, state variables are currents and rotor flux and output is also the current. The induction motor as a state system is defined by (4).

$$\dot{x}(t) = A \cdot x(t) + B \cdot u(t)$$

$$y(t) = C \cdot x(t) \quad (4)$$

Here A is the state matrix, $\boldsymbol{B}$ is the input matrix, $\boldsymbol{C}$ is the output matrix, $\boldsymbol{u}$ is the input, $\boldsymbol{y}$ is the output, and $\boldsymbol{x}$ is the state vector of the system. The system matrixes are defined by (5)

$$A = \begin{bmatrix} -\frac{1}{T_1} & (\frac{k_r}{T_r \cdot L_s'} - j \cdot \frac{k_r \cdot \omega}{L_s'}) \\ \frac{L_m}{T_r} & (-\frac{1}{T_r} + j \cdot \omega) \end{bmatrix},$$

$$B = \begin{bmatrix} \frac{1}{L_s'} \\ 0 \end{bmatrix}, \qquad C = \begin{bmatrix} 1 & 0 \end{bmatrix} \quad (5)$$

and parameters of the motor as (6).

$$R_1 = R_s + R_r \cdot \frac{L_m^{\ 2}}{L_r^{\ 2}}, T_1 = \frac{L_s'}{R_1}, T_r = \frac{L_r}{R_r}, k_r = \frac{L_m}{L_r},$$

$$\sigma = 1 - \frac{L_m^{\ 2}}{L_s \cdot L_r}, L_s' = \sigma \cdot L_s \tag{6}$$

Then the observer system can be defined by (7) as the original system with correction coefficient ***K*** in addition.

$$\dot{\hat{x}}(t) = A \cdot \hat{x}(t) + B \cdot u(t) + K \cdot (y(t) - C \cdot \hat{x}(t)) \tag{7}$$

All the variables calculated by the observer are marked with a circumflex. The matrixes of the observer remain the same as the matrixes in system description and the matrix ***K*** is the correction matrix for the states of the observer. The matrix ***K*** is designed to shift the observer poles to negative real values to ensure the stability of the observer system [7]. The common values of the coefficient were chosen [3], [8].

The matrix A contains angular speed. In this application, the same conditions are applied for both the original model and the observer, so the speed was not measured. Instead, it was treated as parameter and estimated by a PI controller. The control deviation was gained from the difference between measured and estimated current and from estimated flux vector (8). Then the angular speed is calculated according to (9).

$$e(t) = (\hat{i}_{s\alpha} - i_{s\alpha}) \cdot \hat{\psi}_{r\beta} - (\hat{i}_{s\beta} - i_{s\beta}) \cdot \hat{\psi}_{r\alpha} \tag{8}$$

$$\hat{\omega}_r(t) = K_p \cdot e(t) + K_i \cdot \int_0^t e(t)dt \tag{9}$$

The constants K_p and K_i are PI controller coefficients (in this case $K_p = 0.5$; $K_i = 100$). The scheme of the Luenberger observer is shown in Fig. 2.

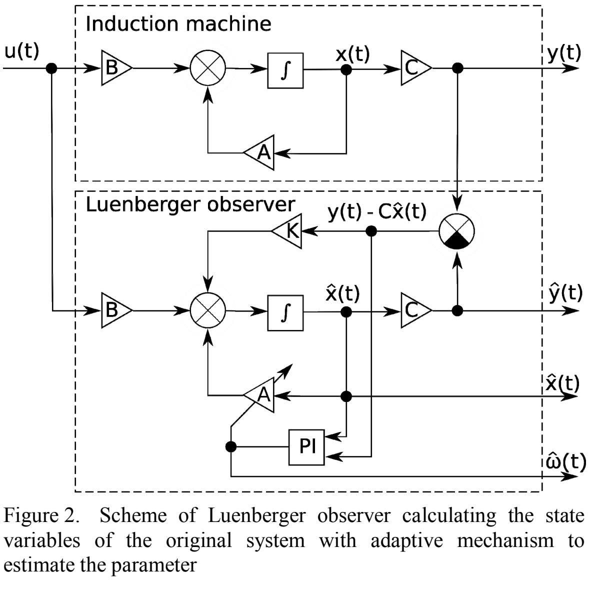

Figure 2. Scheme of Luenberger observer calculating the state variables of the original system with adaptive mechanism to estimate the parameter

Finally, the stator flux vector and torque are calculated from the states according to the induction motor equations (10) and (11).

$$\hat{\psi}_s = (L_s - \frac{L_m^{\ 2}}{L_r}) \cdot \hat{i}_s + \frac{L_m}{L_r} \cdot \hat{\psi}_r \tag{10}$$

$$\hat{T} = \frac{3}{2} \cdot \frac{L_m}{L_r} \cdot p_p \cdot (\hat{\psi}_{r\alpha} \cdot \hat{i}_{s\beta} - \hat{\psi}_{r\beta} \cdot \hat{i}_{s\alpha}) \tag{11}$$

Then the flux sector is determined and its amplitude calculated.

This method requires knowledge of stator resistance R_s, rotor resistance R_r, magnetizing inductance L_m, stator inductance L_s, rotor inductance L_r, and moment of inertia J.

III. Results

The methods were realized on drive with four-pole squirrel cage induction motor of 5.5 kW output power. The IGBT bridge inverter sourced the motor and was controlled by the dSPACE ds1103 platform. The control loop was set to 50 µs. No modulation was used for switching of transistors. They were controlled directly by the control loop. Therefore, the switching frequency was not constant but was changing according to the chosen hysteresis.

In the first measurement, the steady state was tested. The working point was set to constant angular speed of 1000 rpm and the torque reference was set to 30 Nm. The hysteresis was adjusted for each model in order to achieve the same switching frequency. Fig. 3 shows the waveforms of torque and switching frequency for both models. The DTC with Luenberger observer shows better results in smaller torque ripples over the same switching frequency.

In the second measurement, the transient response to the torque reference change was recorded. Fig. 4 shows the torque waveforms and current in one phase of the motor. The waveforms prove that the DTC is able to reach the demanded torque quickly and the utilized model does not make significant difference.

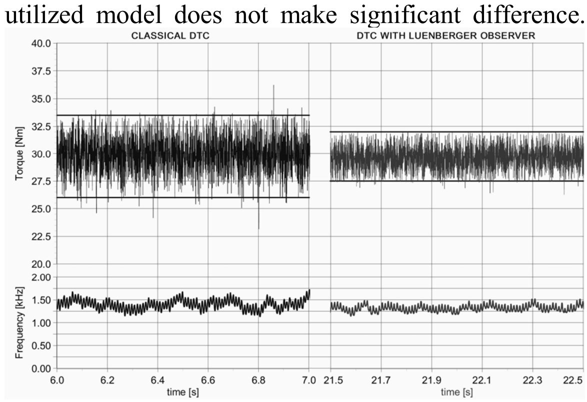

Figure 3. The comparison of torque waveforms with hysteresis control at a 1.5 kHz switching frequency

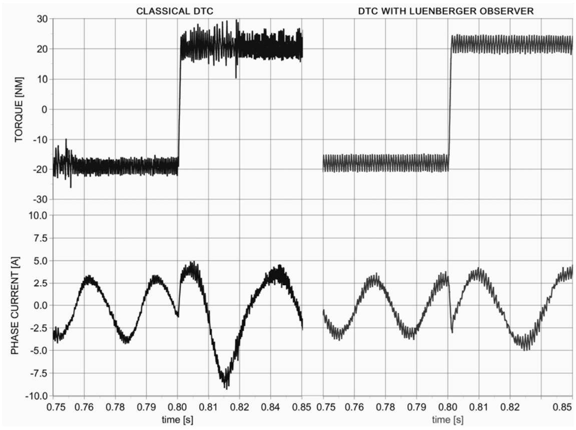

Figure 4. The response of torque and current to a step change in torque.

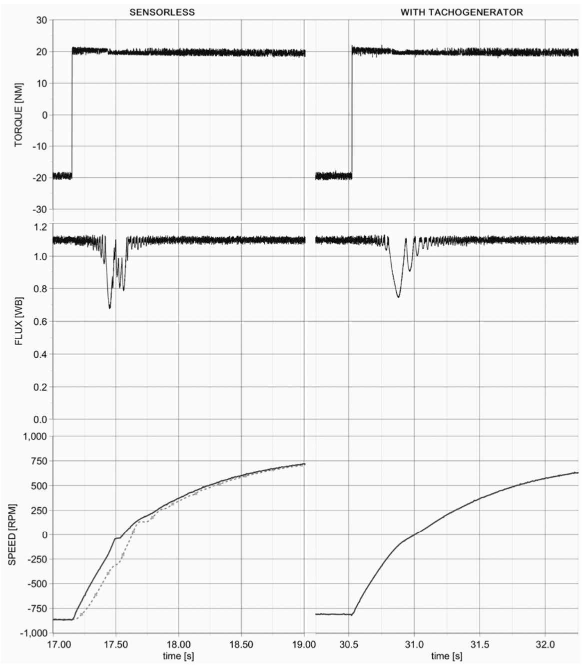

Figure 5. Influence of uncertanities in speed estimation on torque and flux.

The Luenberger observer is utilized to calculate the flux, torque and angular speed of the induction motor. The speed determination is problematic under certain circumstances, such as low speed operation and sudden changes of the speed. The influence of wrong determination of speed on the control ability was tested in the last measurement. The behavior of DTC using Luenberger observer with and without speed sensor were compared at fast changes of speed and during zero crossing. The resulting waveforms are presented in Fig. 5 (the measured speed is plotted in solid line and the estimated speed in dashed line). In the experiment, the speed was reversed using constant torque. The obtained experimental results demonstrate that the torque is very well controlled while the flux amplitude waveform shows bigger divergences.

IV. CONCLUSION

The principles of two different induction motor models used for DTC method were introduced in the paper. Both models (voltage model and Luenberger observer) were implemented on induction motor of 5.5 kW output power using dSPACE ds1103 platform. The same conditions were ensured for both models in term of the sampling time, measured variables, number of sensors, and control loops. The tests were run in different working points and the obtained results were presented and discussed.

The behavior of the drive controlled by DTC with original model and with Luenberger observer in steady states and in transients were examined. The experiments confirmed that in steady states the torque ripple is much smaller while maintaining the same switching frequency. Further it showed that the created model does not have great influence on the transients. At last the experiment showed that the influence of the speed estimation uncertainties does not have a significant impact on the torque accuracy.

ACKNOWLEDGMENT

This material is based on the work supported by the Technology Agency of the Czech Republic under the grant for Competence Centers Program, project No. TE02000103, and on the work supported by the Student Grant Agency of the Czech Technical University in Prague under grant No. SGS16/152/OHK3/2T/13.

REFERENCES

[1] I. Takahashi, T. Noguchi, “A new quick response and high efficiency control strategy of an induction motor”, IEEE Trans. on Ind. Appl., Vol. IA-22, 820 -827, 1986.

[2] A. Chikhi M. Djarallah and K. Chikhi "A comparative study of field-oriented control and direct-torque control of induction motors using an adaptive flux observer" Serbian Journal Of Electrical Engineering vol. 7 no. 1 pp. 41-55 May 2010.

[3] P. Vas, Sensorless vector and direct torque control, Oxford University Press, Oxford,1998.

[4] Z. Xing, Q. Wenlong and Lu Haifeng, "A New Integrator for Voltage Model Flux Estimation in a Digital DTC System," TENCON 2006 - 2006 IEEE Region 10 Conference, Hong Kong, 2006, pp. 1-4.

[5] L. Mihalache, "A flux estimator for induction motor drives based on digital EMF integration with pre- and post- high pass filtering," Twentieth Annual IEEE Applied Power Electronics Conference and Exposition, 2005. APEC 2005., Austin, TX, 2005, pp. 713-718 Vol. 2.

[6] G. Mino Aguilar, G. A. Muñoz Hernandez, J. L. Romeral, L. Cortez and J. Saynes Torres, "Implementation of the direct torque control (DTC) in current model, with current starting limiter," *CONIELECOMP 2012, 22nd International Conference on Electrical Communications and Computers*, Cholula, Puebla, 2012, pp. 278-282.

[7] Franklin, G., F., Powell, J. D., Emami-Naeini, Feedback Control of Dynamic Systems, 7th edition, Pearson, 880 pages, 2014

[8] Y. Zhang, Z. Zhao, T. Lu, L. Yuan, W. Xu and J. Zhu, "A comparative study of Luenberger observer, sliding mode observer and extended Kalman filter for sensorless vector control of induction motor drives," 2009 IEEE Energy Conversion Congress and Exposition, San Jose, CA, 2009, pp. 2466-2473.

[9] T. Kim, H. Shim and D. D. Cho, "Distributed Luenberger observer design," 2016 IEEE 55th Conference on Decision and Control (CDC), Las Vegas, NV, 2016, pp. 6928-693.